Electronic Supplementary Material (ESI) for Journal of Materials Chemistry A.
This journal is © The Royal Society of Chemistry 2024

Supporting Information

Integrating Transition Metal Phosphide Catalysts on WO_3 Photoanodes Enabling Robust Photoelectrocatalytic Water Oxidation †

Biao Yang,‡ Changlong Ru,‡ Yuye Jiao,‡ Lihua Gao, Yurou Song, Zhiqiang Hu and Jungang Hou *

State Key Laboratory of Fine Chemical, Frontiers Science Center for Smart Materials Oriented Chemical Engineering, School of Chemical Engineering, School of Chemistry, Dalian University of Technology, 116024 Dalian, P. R. China. E-mail: jhou@dlut.edu.cn.

‡ These authors contributed equally to this work.

Experimental

Chemical Reagents.

Citric acid anhydrous ($C_6H_8O_7$, 99.5%), hydrogen peroxide (H_2O_2, 30 wt% in H_2O), sodium hypophosphite (NaH_2PO_2, 99.0%), nickel (II) chloride hexahydrate ($NiCl_2 \cdot 6H_2O$, 98.0%), cobalt (II) chloride hexahydrate ($CoCl_2 \cdot 6H_2O$, AR), ferric (III) chloride hexahydrate ($FeCl_3 \cdot 6H_2O$, 99.0%), cobalt (II) nitrate hexahydrate ($Co(NO_3)_2 \cdot 6H_2O$, 99.0%), cobalt (II) sulphate heptahydrate ($CoSO_4 \cdot 7H_2O$, ≥99.0%), copper (II) chloride dihydrate ($CuCl_2 \cdot 2H_2O$, AR), nickel (II) nitrate hexahydrate ($Ni(NO_3)_2 \cdot 6H_2O$, 98.0%), ferric (III) nitrate nonahydrate ($Fe(NO_3)_3 \cdot 9H_2O$, AR), sodium hydroxide (NaOH, 97.0%) were purchased from Aladdin. FTO Glass (SnO_2: F, 1 ×2 cm^2) was bought from Advanced Election Technology Co. Ltd. Ammonium tungstate ($H_{40}N_{10}O_{41}W_{12} \cdot xH_2O$, 85~90%) was purchased from Sinopharm Group. Hydrochloric acid (HCl, 37 wt%) and nitric acid (HNO_3, 68 wt%) were brought from Tianjin Third Chemical Reagent Factory. Ultrapure water (H_2O, 18.2 MΩ) was purchased from Dalian University of Technology.

Preparation of WO_3 photoanode

The WO_3 photoanode was prepared by hydrothermal method.[1] Firstly, dissolved 1.0 g ammonium tungstate in 95 mL deionized water, then added 0.7 mL concentrated hydrochloric acid, and stirred thoroughly. Then, 2 mL hydrogen peroxide and 0.46 g anhydrous citric acid were added to the mixed solution, and the solution was continuously stirred until clear and transparent. Then, the obtained precursor solution was transferred to a Teflon-lined autoclave, the FTO conductive side down immersed in the solution, and heated at 160 ℃ for 5 h. After cooling to room temperature, the electrode was washed by deionized water and dried. Finally, the prepared photoanodes were annealed in air at 500 ℃ for 2 h.

Preparation of MP_x nanoparticles

The Ni_2P cocatalysts were prepared based on reported processes.[2] Specifically, the $NaH_2PO_2 \cdot H_2O$ and $NiCl_2 \cdot 6H_2O$ (molar ratio 5:1) were mixed by grinding, and then the mixture was heated at 250 ℃ for 2 h under nitrogen atmosphere. The black solids obtained were cleaned by centrifugation and dried overnight. The preparation steps of the Cu_3P and Co_2P were similar to the Ni_2P, except that the $NiCl_2 \cdot 6H_2O$ was replaced by the $CoCl_2 \cdot 6H_2O$ and $CuCl_2 \cdot 2H_2O$.

For the preparation of the FeP, the $Fe(NO_3)_3 \cdot 5H_2O$ and NaOH (molar ratio 1:3), excessive NaOH were dissolved in deionized water, stirred for 30 min, and centrifuged with deionized water and ethanol to obtain the $Fe(OH)_3$ precipitate. The $Fe(OH)_3$ and $NaH_2PO_2 \cdot H_2O$ were mixed at the molar ratio of 5:1, and the resulting mixture was calcined at 300 ℃ in nitrogen atmosphere for 2 h. The black solids obtained were cleaned by centrifugation and dried overnight.

Construction of WO_3/MP_x photoanode

The obtained MP_x particles were ultrasonic dispersed in anhydrous ethanol (the concentration was 1.0~5.0 mg mL^{-1}), then the suspension was loaded onto the surface of the WO_3 photoanode through spin coating (1000 rpm), and finally annealed at 120 ℃ in air for 2 h to obtain the WO_3/MP_x photoanode.

Construction of WO_3/OECs photoanode

The WO_3/NiOOH photoanode was prepared by electrodeposition.[3] The electrodeposited solution was 0.1 M $NiSO_4$ (using 1 M NaOH solution to adjust the pH = 6.5-7.2. The photodeposition was first carried out under simulated solar illumination of AM 1.5 G (100 mW cm^{-2}) at 0.15 V vs. Ag/AgCl for 10 min. Subsequently, the photoanodes were deposited for 1 min at 1.23 V vs. Ag/AgCl under dark conditions, then washed and dried.

The WO_3/Ni-Pi photoanode was prepared by the reported method.[4] The electrodeposition solution was prepared by dissolving 0.2 M $Ni(NO_3)_2$ $6H_2O$ in 0.5 M phosphate buffer (pH ≈ 7), and then deposited for 200 s under simulated solar illumination of AM 1.5 G (100 mW cm^{-2}) and 0.2 V vs. Ag/AgCl. The obtained photoanodes were rinsed with deionized water and dried.

Characterization

Scanning electron microscope (SEM, JSM-7900F), transmission electron microscope (TEM) and energy dispersive spectrometer (EDS) characterizations were used for morphology and elemental analysis. X-ray photoelectron spectrometer (XPS) with an ESCALAB 250Xi analyzer using monochromatic Al Kα radiation (225 W, 15 mA, 15 kV), powder X-ray diffraction (XRD, a Bruker D8 advance diffractometer with Cu Kα radiation) were adopted to characterize the as-prepared samples. Ultraviolet–visible (UV-vis, UV-3600 Plus) absorption and photoluminescence/time-resolved transient photoluminescence decay (PL/TRPL, FLS 1000 fluorescence spectrometer with both continuous (450 W) and pulsed Xenon lamps) measurements were carried out to record the optical properties of samples. Raman spectroscopy (DXR Microscope) was used for structural confirmation of samples. Surface photovoltage spectroscopy (SPV, CEL-SPS1000) was used to test photogenerated carrier separation.

Measurements of Photoelectrochemical (PEC) Performance

The PEC measurements were carried out on an electrochemical workstation (CH Instruments, CHI 660E) with a three-electrode system. WO_3 based photoanodes were utilized as the working electrodes, Pt wire as the counter electrode and Ag/AgCl electrode as the reference electrode, respectively. The 0.5 M Na_2SO_4 electrolyte (pH = 6.9) was used for WO_3 photoanodes. All the photoanodes with working area of 1 cm^2 were irradiated by simulated sunlight (100 mW cm^{-2}, 300 W Xe lamp with AM 1.5 G filter). The linear sweep voltammery (LSV) was proceeded with a scanning rate of 0.05 V s^{-1} under a potential from 0.4 V to 1.4 V versus reversible hydrogen electrode (vs. RHE). The potential vs. RHE (E_{RHE}) was calibrated using the Nernst equation:

$$E_{RHE} = E_{\mathrm{Ag/AgCl}} + 0.059 \times \mathrm{pH} + E^{0}_{\mathrm{Ag/AgCl}} \quad (1)$$

where $E_{\mathrm{Ag/AgCl}}$ is the applied potential vs. Ag/AgCl electrode and $E^{0}_{\mathrm{Ag/AgCl}}$ is 0.197 V at 25 ℃.

The electrochemical impedance spectroscopy (EIS) were measured via the electrochemical workstation (frequency of 0.01 Hz to 100 kHz).

Incident Photon-to-Electron Conversion Efficiencies (IPCE) Calculation

IPCE spectra were obtained by calculation at each monochromatic wavelength according to the following equation:

$$\mathrm{IPCE}(\%) = \left[\frac{1240 \times J_{light}}{\lambda \times P_{light}}\right] \times 100\% \quad (2)$$

where λ, J_{light}, and P_{light} are the wavelength (nm) of incident light, the photocurrent density under corresponding λ and the irradiance intensity (mW cm^{-2}) of incident light, respectively.

Applied bias photon-to-current efficiency (ABPE) Calculation

ABPE curves were derived from the following equation:

$$\text{ABPE}(\%) = [\frac{(1.23-V_s) \times (J_{light} - J_{dark})}{P_{light}}] \times 100\% \quad (3)$$

where V_s is the applied bias versus RHE, P_{light} is the incident light intensity (100 mW cm^{-2}), J_{light} and J_{dark} are the current densities (mW cm^{-2}) measured under AM 1.5 G illumination and dark conditions, respectively.

Mott-Schottky Measurements

To further detect the photogenerated carrier recombination behavior, the Mott-Schottky measurement was carried out. The capacitance was obtained by the expression:

$$\frac{1}{C_{SC^2}} = \frac{2}{eN_dA^2\varepsilon\varepsilon_0} \times (E - E_{fb} - \frac{TK_B}{e}) \quad (4)$$

$$N_d = \frac{2}{e\varepsilon\varepsilon_0} \times [\frac{d(1/C^2)}{dV_S}]^{-1} \quad (5)$$

where C_{SC} is the capacitance of space charge layer (obtained from MS curves), Vs is the applied potential, ε_0 is the vacuum permittivity (8.86 × 10^{-12} F m^{-1}), ε is the dielectric constant of semiconductor, A is the working area of photoanode (1 cm^2), e is the electronic charge (1.6 × 10^{-19} C), N_d is the carrier density, E_{fb} is the flat-band potential, K_B is the Boltzmann constant (1.38 × 10^{-23} J K^{-1}), T is the temperature.

Current-Time Curves

The stability of different photoanodes can be evaluated by current-time curves (i-t). A long-time current density test was performed under simulated solar illumination at AM 1.5 G (100 mW cm^{-2}) at 1.23 V vs. RHE.

Charge Transfer Efficiency (η_{trans}) Calculation

The charge transfer (η_{trans}) efficiency was calculated according to the equations below:

$$\eta_{trans} = \frac{J_{H_2O}}{J_{Na_2SO_3}} \times 100\% \quad (6)$$

where J_{H_2O} is the measured photocurrent density without Na_2SO_3 hole scavengers in the electrolyte, $J_{Na_2SO_3}$ is the photocurrent density with 0.2 M Na_2SO_3 hole scavengers in the electrolyte.

Faraday Efficiency Calculation

In photoelectrocatalytic systems, the Faraday efficiency (FE%) is commonly used to evaluate the performance of catalysts, it was calculated according to the equations below:

$$\text{FE}(\%) = \frac{Q_{product}}{Q_{total}} = \frac{n \times F \times N_{product}}{J \times A \times t} \quad (7)$$

where n is the number of electrons transferred during the reaction, F is Faraday constant (96485 C mol^{-1}), $N_{product}$ is the molar amount of product actually produced (mol), J is the measured optical current density (mA cm^{-2}), A is the working area of photoanode (1 cm^2), t is the reaction time (s).

Fitting of Time-Resolved Transient Photoluminescence Lifetime

Biexponential function fitting was employed to analyze the time-resolved photoluminescence decay curves:

$$L(t) = A_1 e^{\left(\frac{-t}{\tau_1}\right)} + A_2 e^{\left(\frac{-t}{\tau_2}\right)} + y_0 \quad (8)$$

The average carrier lifetime (τ_{ave}) was calculated by the following :

$$\tau_{ave} = \frac{A_1\tau_1^2 + A_2\tau_2^2}{A_1\tau_1 + A_2\tau_2} \quad (9)$$

where τ_1 and τ_2 are defined as the decay time for the fluorescence intensity, representing the speed of carrier recombination. The fitting parameters are given in Table S2.

Table S1. Fitting EIS data and N_d of WO_3, WO_3/Co_2P, WO_3/FeP, WO_3/Cu_3P, WO_3/Ni-Pi, WO_3/NiOOH and WO_3/Ni_2P photoanodes.

Samples (photoanodes)	R_s (Ω)	R_{ct} (Ω)	N_d (cm^{-3})
WO_3	32.16	1781	1.17×10^{22}
WO_3/Co_2P	32.42	876.9	2.44×10^{22}
WO_3/FeP	30.85	670.6	3.75×10^{22}
WO_3/Cu_3P	30.99	584.6	5.05×10^{22}
WO_3/Ni-Pi	31.08	767.9	1.64×10^{8}
WO_3/NiOOH	31.43	651.9	4.69×10^{22}
WO_3/Ni_2P	30.43	499.6	7.04×10^{22}

Table S2. Biexponential decay-fitted parameters of TRPL decay curves for WO_3 and WO_3/MP_x photoanodes.

Samples (photoanodes)	τ_1 (ns)	A_1	τ_2 (ns)	A_2	τ_{ave} (ns)
WO_3	0.82	0.90	10.18	0.52	9.03
WO_3/Co_2P	0.95	0.95	16.71	0.43	14.95
WO_3/FeP	1.01	0.50	18.33	0.47	17.37
WO_3/Cu_3P	1.53	0.34	25.01	0.44	23.95
WO_3/Ni_2P	2.02	1.05	30.86	0.56	27.71

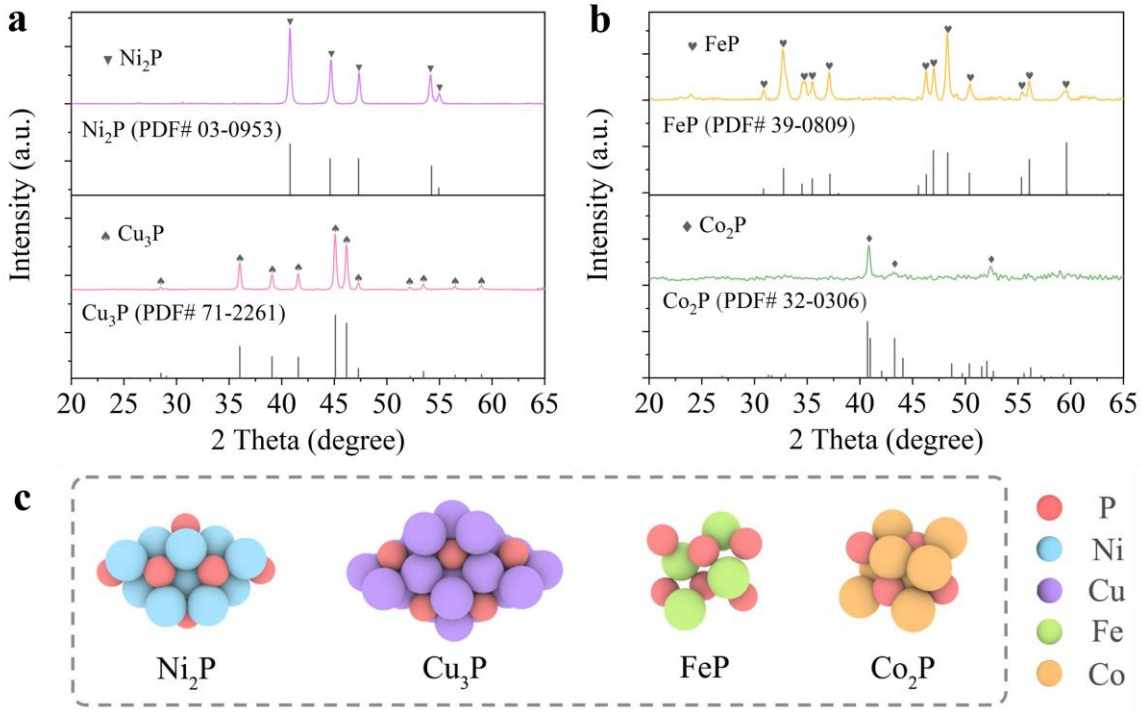

Fig. S1 XRD patterns of and (a, b) MP_x nanoparticles. (c) Structure diagram of MP_x nanoparticles.

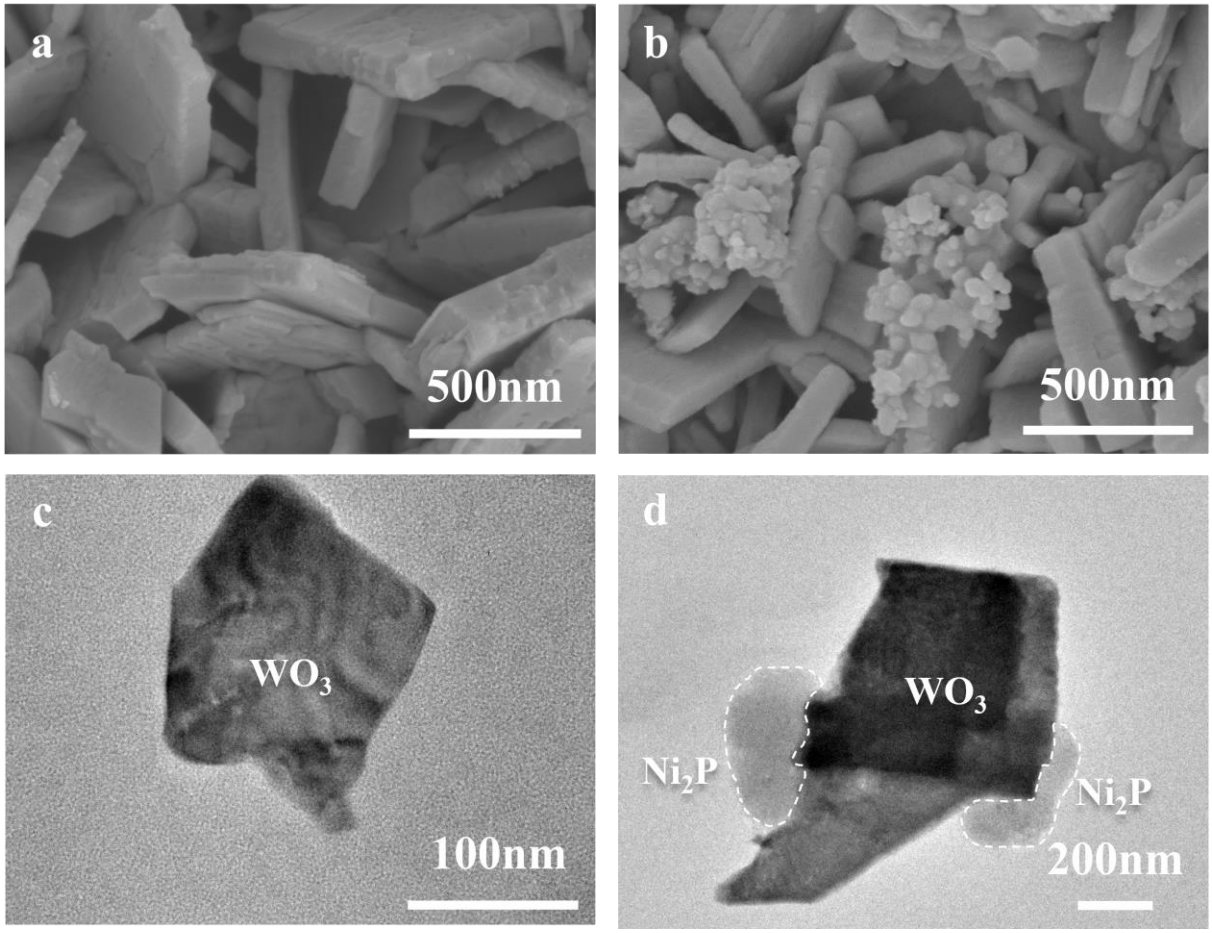

Fig. S2 (a) Top-view SEM image of WO_3 photoanode, (b) top-view SEM images of WO_3/Ni_2P photoanode. (c) TEM image of WO_3 photoanode, (d) TEM image of WO_3/Ni_2P photoanode.

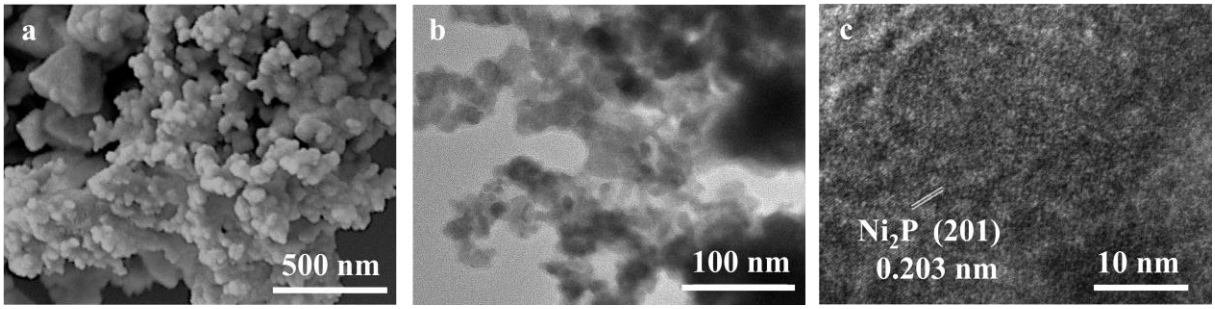

Fig. S3 (a) Top-view SEM image of Ni_2P, (b) and (c) TEM images of Ni_2P catalyst.

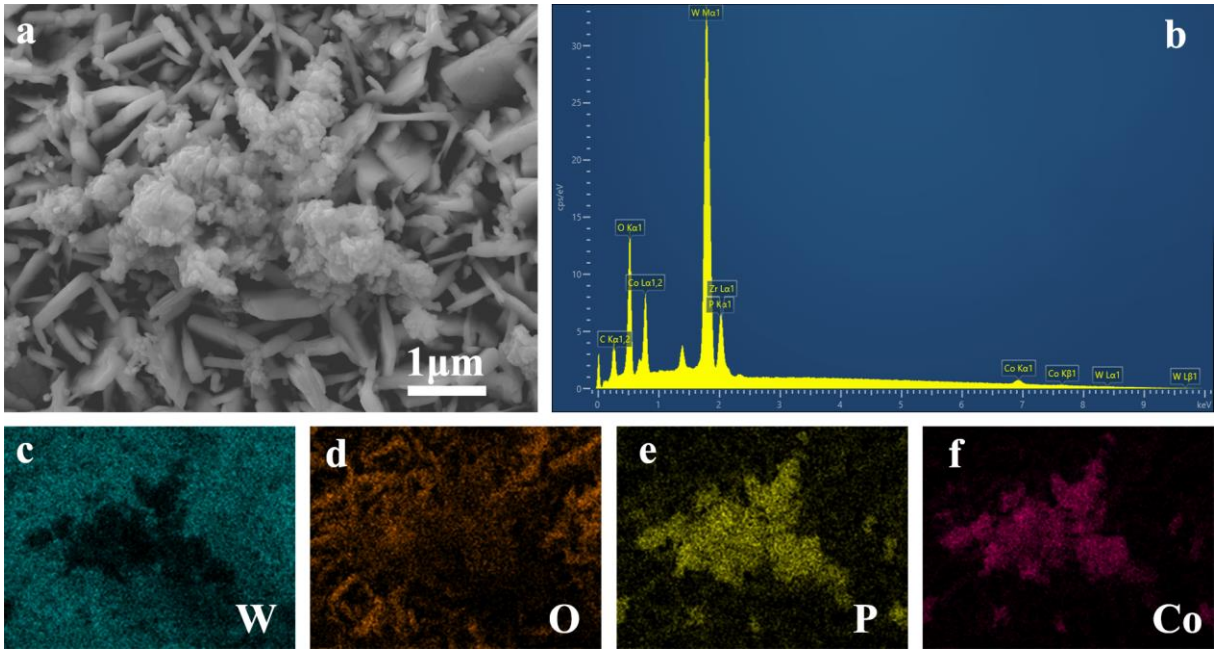

Fig. S4 (a) SEM and (b-f) EDS images of WO_3/Co_2P photoanode.

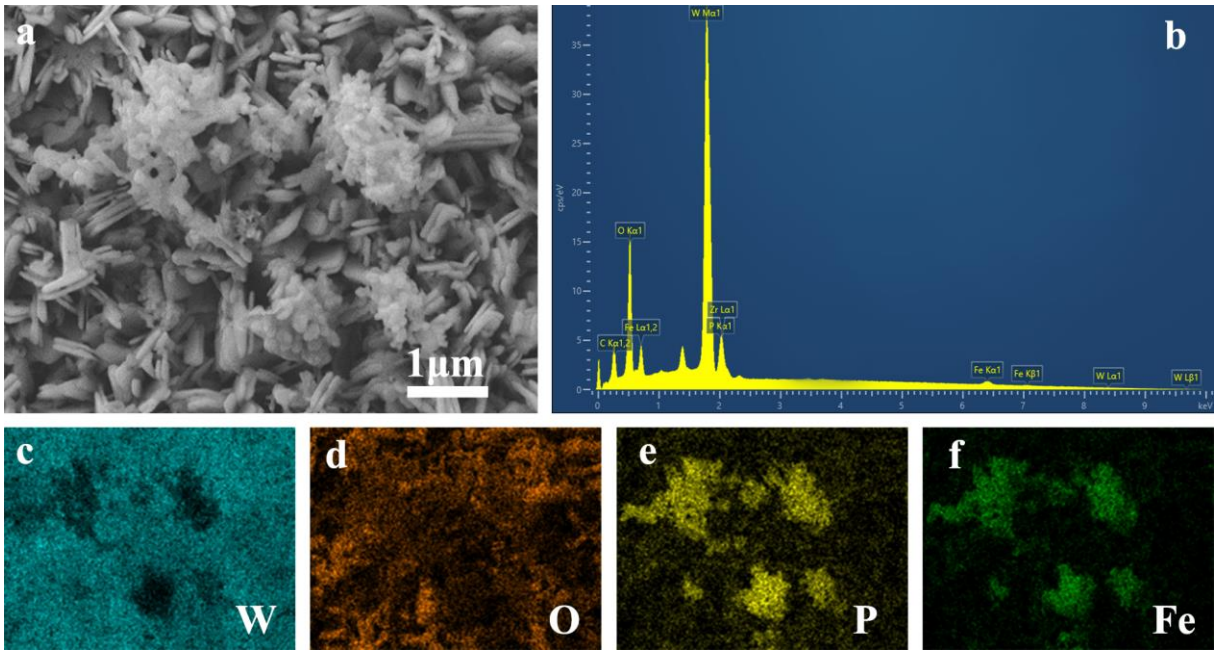

Fig. S5 (a) SEM and (b-f) EDS images of WO_3/FeP photoanode.

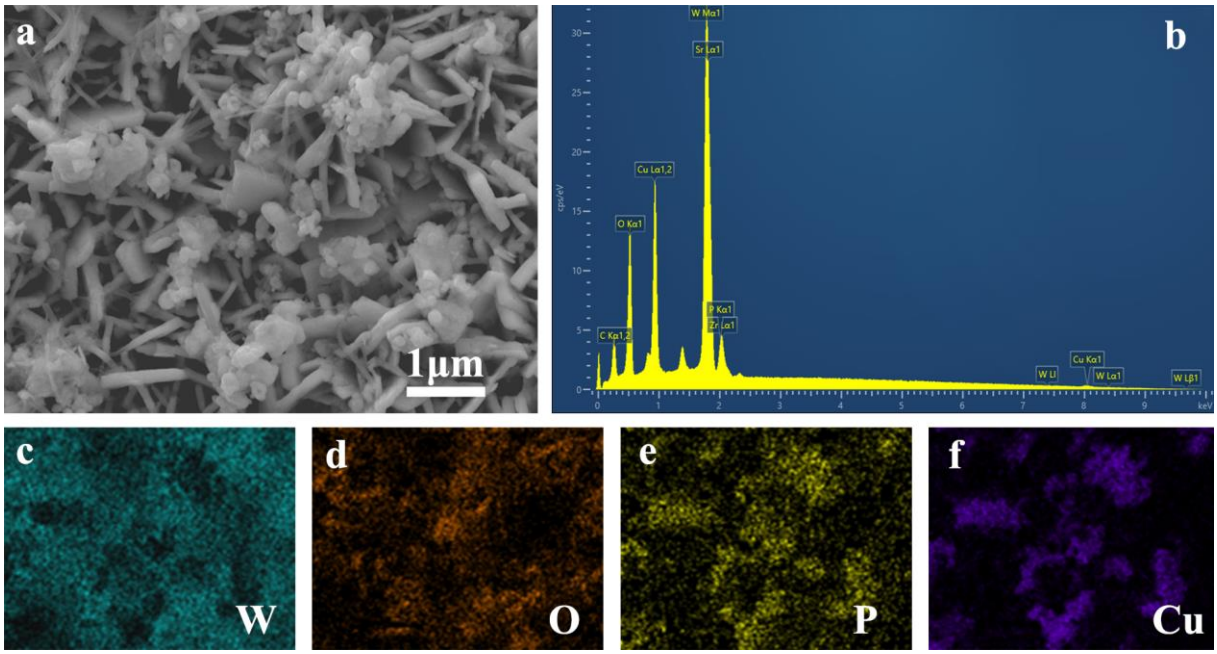

Fig. S6 (a) SEM and (b-f) EDS images of WO_3/Cu_3P photoanode.

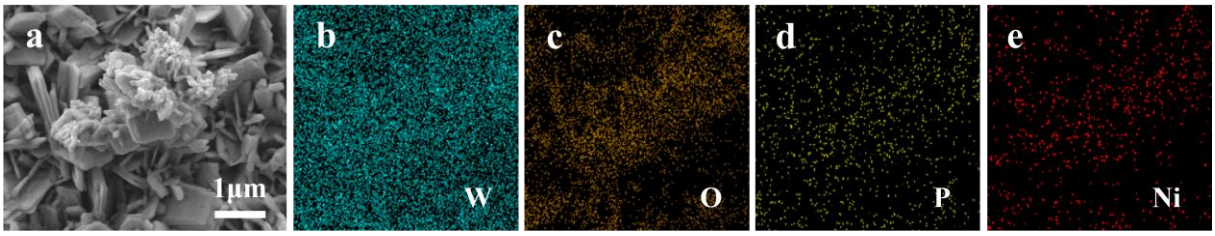

Fig. S7 (a) SEM and (b-e) EDS images of WO_3/Ni_2P photoanode after the reaction.

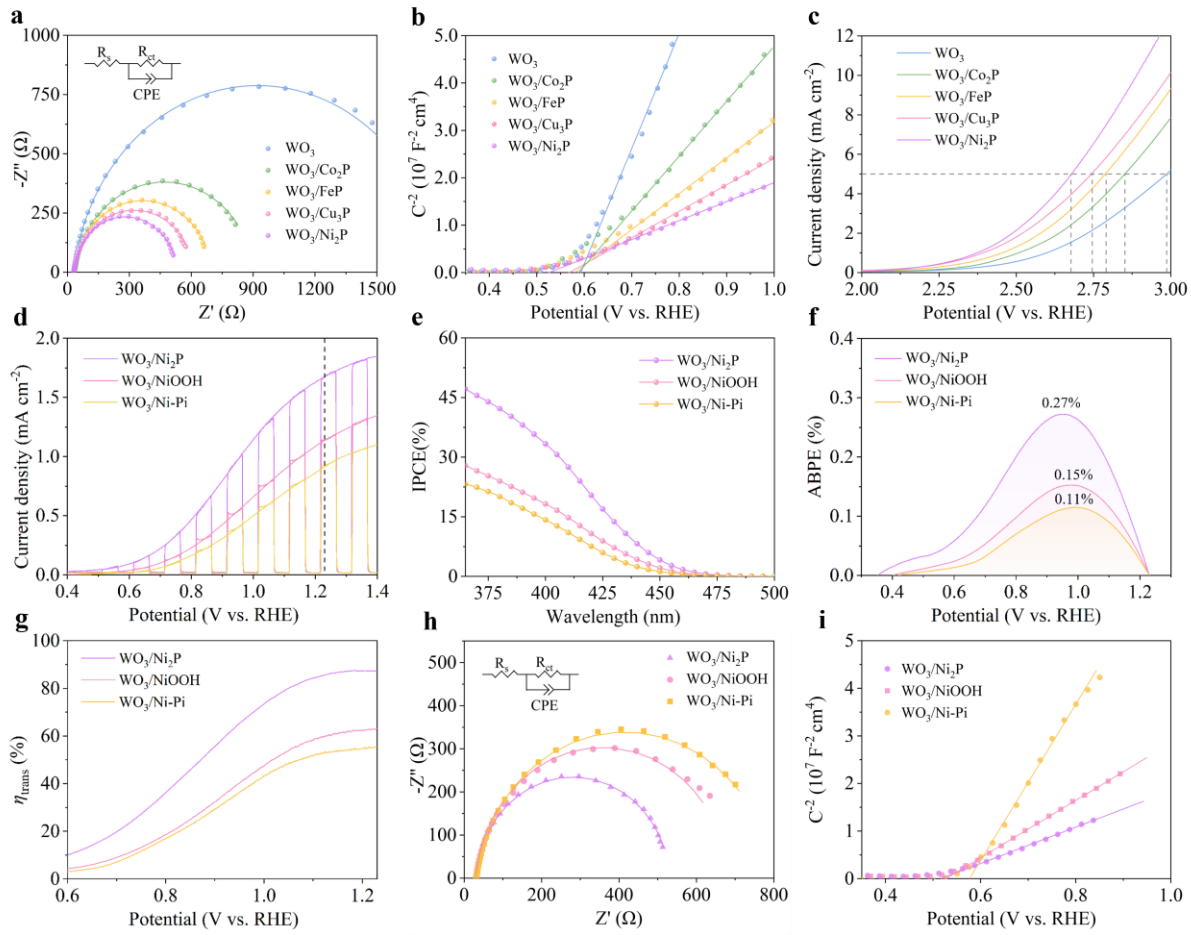

Fig. S8 (a) EIS curves, (b) M-S plots, and (c) LSV curves in darkness of WO_3 and WO_3/MP_x photoanodes, (d) LSV curves, (e) IPCE curves measured at 1.23 V vs. RHE, (f) ABPE curves, (g) η_{trans} curves, (h) EIS curves and (i) M-S plots of WO_3/Ni_2P, WO_3/NiOOH and WO_3/Ni-Pi photoanodes.

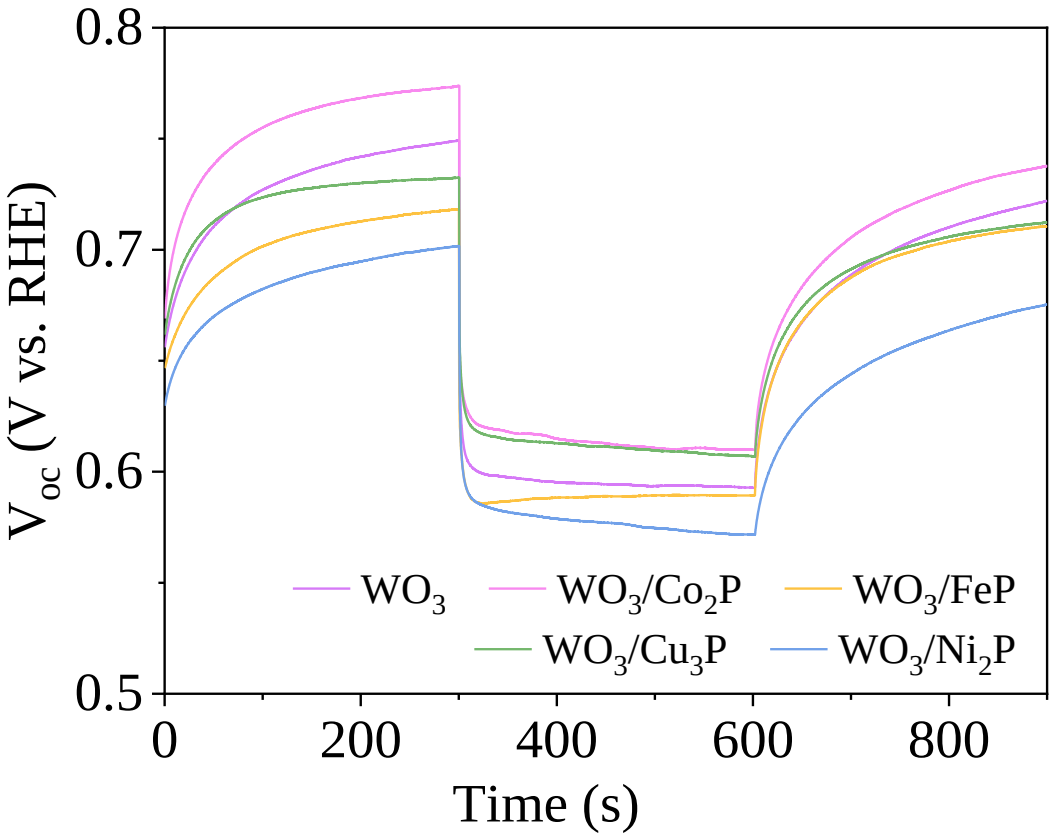

Fig. S9 The OCP transient decay curves of WO_3 and WO_3/MP_x photoanodes after passing oxygen for 30 min prior to the test and extending the test time.

References

1. X. Y. Feng, Y. B. Chen, Z. X. Qin, M. L. Wang and L. J. Guo, *ACS Appl. Mater. Inter.*, 2016, **8**, 18089-18096.
2. L. A. Stern, L. G. Feng, F. Song and X. L. Hu, *Energ. Environ. Sci.*, 2015, **8**, 2347-2351.
3. L. F. Li, S. N. Xiao, R. P. Li, Y. N. Cao, Y. Chen, Z. C. Li, G. S. Li and H. X. Li, *ACS Appl. Energ. Mater.*, 2018, **1**, 6871-6880.
4. Z. C. Hao, Z. F. Liu, Y. T. Li, M. N. Ruan and Z. G. Guo, *Int. J. Hydrogen Energ.*, 2020, **45**, 16550-16559.